FREE VIBRATION ANALYSIS OF FUNCTIONALLY GRADED DOUBLY-CURVED SHALLOW SHELLS INCLUDING THERMAL EFFECT

Duong Thanh Huan[1*], Tran Huu Quoc[2], Tran Minh Tu[2], Le Minh Lu[1]

[1]Faculty of Engineering, Vietnam National University of Agriculture
[2]National University of Civil Engineering

Email[*]: dthuan@vnua.edu.vn

Ngày gửi bài: 30.08.2017 Ngày chấp nhận: 03.11.2017

ABSTRACT

In this paper, theoretical formulation, Navier's solutions, and finite element models based on the first-order shear deformation shell theory are presented for the free vibration analysis of functionally graded doubly-curved shallow shell panels including thermal effects. The temperature field was considered to have a uniform distribution over the shell surface and varied in the thickness direction only. The material properties were assumed to be temperature-dependent, and graded in the thickness direction according to a simple power law distribution in terms of the volume fractions of the constituents. All four edges of the shell panels were assumed to be simply supported. Comparisons reveal that the numerical results obtained from the proposed method agree well with those available in the literature. The effects of the side-to-thickness ratio (a/h), temperature fields (T_c), and volume fraction distribution (p) on the natural frequencies of the functionally graded doubly-curved shallow shell panels were also investigated in the present study.

Keywords: Functionally graded materials (FGM), free vibration analysis, FSDT, FEM, thermal environment, doubly-curved shells.

Phân tích dao động riêng vỏ thoải hai độ cong có cơ tính biến thiên kể đến ảnh hưởng của nhiệt độ

TÓM TẮT

Bài báo trình bày lời giải giải tích và mô hình phần tử hữu hạn trên cơ sở lý thuyết vỏ bậc nhất (5 ẩn số chuyển vị) cho bài toán phân tích dao động riêng vỏ thoải hai độ cong có cơ tính biến thiên và có xét đến ảnh hưởng của nhiệt độ. Trường nhiệt độ được xét đến là phân bố đều trên các bề mặt vỏ và chỉ biến thiên theo phương chiều dày vỏ. Các cơ tính của vật liệu FGM được giả thiết phụ thuộc vào nhiệt độ và thay đổi dọc theo phương chiều dày với quy luật của hàm lũy thừa. Các đối tượng vỏ được khảo sát với điều kiện biên tựa khớp trên tất cả các cạnh. Kết quả số đã được kiểm chứng với kết quả của các tác giả khác cho thấy sự tương đồng cũng như độ tin cậy của hai lời giải đề xuất trong nghiên cứu này. Mặt khác, ảnh hưởng của tỉ số kích thước cạnh/chiều dày vỏ (a/h), trường nhiệt độ (T_c) và chỉ số tỉ lệ thể tích vật liệu (p) đến giá trị tần số dao động riêng của vỏ thoải hai độ cong cũng đã được khảo sát thông qua các ví dụ số.

Từ khóa: Vật liệu có cơ tính biến thiên (FGM), phân tích dao động riêng, lý thuyết biến dạng cắt bậc nhất (FSDT), phương pháp phần tử hữu hạn, môi trường nhiệt, vỏ hai độ cong.

1. INTRODUCTION

Functionally graded materials (FGMs) are frequently used in engineering communities, especially in applications for high-temperature environments such as nuclear reactors, space planes, and chemical plants. Typical FGMs are made from a mixture of ceramic and metal, or a combination of different metals. The ceramic constituent

provides high-temperature resistance due to its low thermal conductivity. The ductile metal constituent, on the other hand, prevents fractures caused by stresses due to a high-temperature gradient over a very short period of time. There are numerous studies on the thermo-mechanical characteristics of FGM structures which have been carried out to date.

Generally, the studies of static and dynamic analyses of functionally graded shells working in thermal environments are well-established throughout the literature. Kadoli and Ganesan (2006) presented a linear thermal buckling and free vibration analyses for functionally graded cylindrical shells with clamped-clamped boundary conditions and with temperature-dependent material properties. The first-order shear deformation theory along with the Fourier series expansion of the displacement variables in the circumferential direction were used to model the FGM shell. Shen and Wang (2010) investigated the thermoelastic vibration and buckling characteristics of the functionally graded piezoelectric cylindrical shell using the Maxwell equation with a quadratic variation of the electric potential along the thickness direction of the cylindrical shells and the first-order shear deformation theory. Based on Love's shell theory and the von Karman-Donnell-type of kinematic nonlinearity, free vibration analysis of simply supported FG cylindrical shells for four sets of in-plane boundary conditions was performed by Haddadpour *et al.* (2007) using Galerkin's method. The free vibration analysis of rotating functionally graded (FG) cylindrical shells subjected to thermal environment was investigated based on the first order shear deformation theory of shells and was reported in the work of Malekzadeh and Heydarpour (2012). Pradyumna and Bandyopadhyay (2010) investigated the free vibration and buckling behaviors of functionally graded singly and doubly curved shell panels in thermal environments. A higher-order shear deformation theory was used and the shell panels were subjected to a temperature field. Bhangale *et al.* (2006) used the first-order shear deformation theory to study the thermal buckling and vibration behaviors of truncated FGM conical shells in a high-temperature environment by the finite element method. Temperature-dependent material properties were considered to carry out linear thermal buckling and free vibration analyses. Zhao and Liew (2009) studied the static response and free vibration characteristics of metal and ceramic functionally graded shells using the element-free kp-Ritz method. The displacement field was expressed in terms of a set of mesh-free kernel particle functions according to Sander's first-order shear deformation shell theory. Wattanasakulpong and Chaikittiratana (2015) presented an investigation of free vibration of stiffened functionally graded doubly curved shallow shells under a thermal environment. Two types of temperature icreases, linear and nonlinear, were considered throughout the shell thickness. Alijani *et al.* (2011) studied geometrically nonlinear vibrations of functionally graded doubly curved shells subjected to thermal variations and harmonic excitation via the doubly-modal energy approach.

Recently, there have been many local authors who have studied this issue. Quan and Duc (2016), using Reddy's third-order shear deformation shell theory, investigated nonlinear vibration and dynamic responses of imperfect functionally graded materials (FGM) using thick double-curved shallow shells resting on elastic foundations in thermal environments. Duc *et al.* (2017) proposed an analytical approach by using the Galerkin method to study the nonlinear dynamics and vibration of S-FGM spherical shallow shells with different types of boundary conditions resting on EF in a thermal environment. A third-order shear deformation theory was used by Dong and Dung (2017) for the nonlinear vibration analysis of stiffened functionally graded material, sandwiched doubly, curved shallow shells with four material models. It can be seen clearly that most of these studies refer to a nonlinear analysis of the doubly-curved shells by using an analytical approach.

However, studies on the free vibration analysis of FGM doubly-curved shell panels in a thermal environment are rare in the literature. Thus, for study purposes in this paper, an analytical solution and finite element model based on the first-order shear deformation theory were used for the free vibration analysis of three shell panels, namely, cylindrical (CYL), spherical (SPH), and hyperbolic paraboloidal (HYP) in thermal a environment.

2. THEORITICAL FORMULATION

In the present study, the shell panels are denoted length a, width b, and thickness h, and are referred to using an orthogonal curvilinear coordinate system (x, y, z), as shown in Fig. 1. R_x and R_y are the radius of principal curvatures of the middle surface in the x-direction and y-direction, respectively. The elastic material properties vary throughout the shell thickness according to the volume fractions of the constituents. The top surface ($z = h/2$) of the shell is assumed ceramic-rich, whereas the bottom surface ($z = -h/2$) is metal rich. The effective properties of the functionally graded material at any thickness coordinate z can be expressed following a power law distribution as

$$P(z,T) = (P_c - P_m)\left(\frac{z}{h} + \frac{1}{2}\right)^p + P_m \quad (1)$$

where p is the volume fraction exponent, and P_m and P_c represent the properties of the metal and ceramic, respectively. The properties of the temperature-dependent constituents of the constituent materials are the same as presented by Yang and Shen (2001):

$$P(T) = P_0\left(P_{-1}T^{-1} + 1 + P_1T + P_2T^2 + P_3T^3\right) \quad (2)$$

where P_0, P_{-1}, P_1, P_2 and P_3 are the coefficients of temperature *T(K)* and are unique to the constituent materials.

In the present analysis, Young's modulus E and thermal expansion coefficient α are assumed to be temperature-dependent, whereas the mass density ρ and thermal conductivity κ are independent to the temperature. The Poisson ratio v is assumed to be constant [10]:

$$E(z,T) = E_m(T) + \left[E_c(T) - E_m(T)\right]\left(\frac{z}{h} + \frac{1}{2}\right)^p;\ \kappa(z) = \kappa_m + (\kappa_c - \kappa_m)\left(\frac{z}{h} + \frac{1}{2}\right)^p;$$
$$\alpha(z,T) = \alpha_m(T) + \left[\alpha_c(T) - \alpha_m(T)\right]\left(\frac{z}{h} + \frac{1}{2}\right)^p;\ \rho(z) = \rho_m + (\rho_c - \rho_m)\left(\frac{z}{h} + \frac{1}{2}\right)^p. \quad (3)$$

We assumed that the temperature variation occurs in the thickness direction only and the one-dimensional temperature field is constant in the XY plane of the shell. In such a case, the temperature distribution throughout the thickness of the FGM shell can be obtained by solving a steady-state heat transfer equation as follows:

$$-\frac{d}{dZ}\left[\kappa(z)\frac{dT}{dZ}\right] = 0 \quad (4)$$

This equation is solved by imposing boundary conditions of $T = T_c$ at $Z = h/2$ and $T = T_m$ at $Z = -h/2$. The solution of this equation, by means of a polynomial series, is [11]:

$$T(z) = T_m + (T_c - T_m)\eta(z) \quad (5)$$ with

$$\eta(z) = \frac{1}{C}\left[X - \frac{\kappa_{cm}}{(p+1)\kappa_m}X^{p+1} + \frac{\kappa_{cm}^2}{(2p+1)\kappa_m^2}X^{2p+1} - \frac{\kappa_{cm}^3}{(3p+1)\kappa_m^3}X^{3p+1} + \frac{\kappa_{cm}^4}{(4p+1)\kappa_m^4}X^{4p+1} - \frac{\kappa_{cm}^5}{(5p+1)\kappa_m^5}X^{5p+1}\right] \quad (6a)$$

$$\begin{cases} X = \left(\dfrac{z}{h} + \dfrac{1}{2}\right); \quad \kappa_{cm} = \kappa_c - \kappa_m \\ C = 1 - \dfrac{\kappa_{cm}}{(p+1)\kappa_m} + \dfrac{\kappa_{cm}^2}{(2p+1)\kappa_m^2} - \dfrac{\kappa_{cm}^3}{(3p+1)\kappa_m^3} + \dfrac{\kappa_{cm}^4}{(4p+1)\kappa_m^4} - \dfrac{\kappa_{cm}^5}{(5p+1)\kappa_m^5} \end{cases} \tag{6b}$$

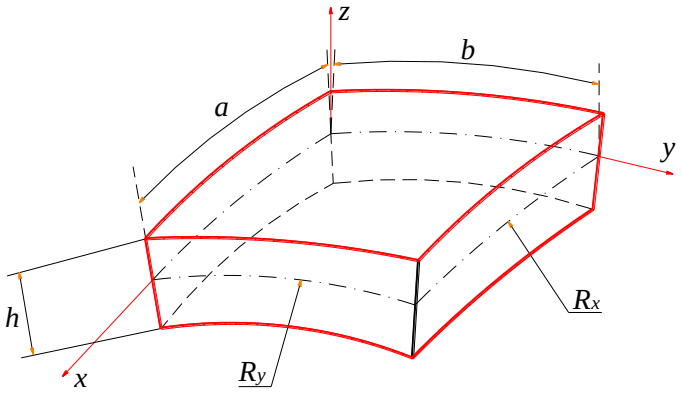

Figure 1. A functionally graded doubly curved shallow shell

According to the first-order shear deformation shell theory, the displacement field can be expressed as

$$\begin{aligned} u(x,y,z,t) &= u_0(x,y,t) + z\phi_x(x,y,t) \\ v(x,y,z,t) &= v_0(x,y,t) + z\phi_y(x,y,t) \\ w(x,y,z,t) &= w_0(x,y,t) \end{aligned} \tag{7}$$

where u_0, v_0, and w_0 are the displacements at the mid-surface of the shell in the x, y, and z directions, respectively, and ϕ_x and ϕ_y represent the rotations of the transverse normal about the x and y axes, respectively.

The linear strains are defined as:

$$\begin{Bmatrix} \varepsilon_x \\ \varepsilon_y \\ \gamma_{xy} \end{Bmatrix} = \begin{Bmatrix} \varepsilon_x^0 \\ \varepsilon_y^0 \\ \gamma_{xy}^0 \end{Bmatrix} + z\begin{Bmatrix} \kappa_x \\ \kappa_y \\ \kappa_{xy} \end{Bmatrix}; \quad \begin{Bmatrix} \gamma_{yz} \\ \gamma_{xz} \end{Bmatrix} = \begin{Bmatrix} \gamma_{yz}^0 \\ \gamma_{xz}^0 \end{Bmatrix} = \begin{Bmatrix} \phi_y + \dfrac{\partial w_0}{\partial y} - \dfrac{v_0}{R_y} \\ \phi_x + \dfrac{\partial w_0}{\partial x} - \dfrac{u_0}{R_x} \end{Bmatrix} \tag{8}$$

where

$$\begin{aligned} &\varepsilon_x^0 = \frac{\partial u_0}{\partial x} + \frac{w_0}{R_x}; \varepsilon_y^0 = \frac{\partial v_0}{\partial y} + \frac{w_0}{R_y}; \gamma_{xy}^0 = \frac{\partial u_0}{\partial y} + \frac{\partial v_0}{\partial x} \\ &\kappa_x = \frac{\partial \phi_x}{\partial x}; \kappa_y = \frac{\partial \phi_y}{\partial y}; \kappa_{xy} = \frac{\partial \phi_x}{\partial y} + \frac{\partial \phi_y}{\partial x} \end{aligned} \tag{9}$$

Then, the linear constitutive relations are expressed as

$$\begin{Bmatrix} \sigma_{xx} \\ \sigma_{yy} \\ \sigma_{xy} \\ \sigma_{yz} \\ \sigma_{xz} \end{Bmatrix} = \begin{bmatrix} Q_{11} & Q_{12} & 0 & 0 & 0 \\ Q_{12} & Q_{22} & 0 & 0 & 0 \\ 0 & 0 & Q_{66} & 0 & 0 \\ 0 & 0 & 0 & Q_{44} & 0 \\ 0 & 0 & 0 & 0 & Q_{55} \end{bmatrix} \begin{Bmatrix} \varepsilon_x \\ \varepsilon_y \\ \gamma_{xy} \\ \gamma_{yz} \\ \gamma_{xz} \end{Bmatrix} \tag{10}$$

where

$$Q_{11}=Q_{22}=\frac{E(z,T)}{1-\nu^2};Q_{12}=\frac{\nu E(z,T)}{1-\nu^2};Q_{44}=Q_{55}=Q_{66}=\frac{E(z,T)}{2(1+\nu)} \qquad (11)$$

The total in-plane force resultants, total moment resultants, and transverse force resultants are defined by:

$$\begin{Bmatrix}N_{xx}\\N_{yy}\\N_{xy}\end{Bmatrix}=\int_{-h/2}^{h/2}\begin{Bmatrix}\sigma_{xx}\\\sigma_{yy}\\\tau_{xy}\end{Bmatrix}dz;\begin{Bmatrix}M_{xx}\\M_{yy}\\M_{xy}\end{Bmatrix}=\int_{-h/2}^{h/2}\begin{Bmatrix}z\sigma_{xx}\\z\sigma_{yy}\\z\tau_{xy}\end{Bmatrix}dz;\begin{Bmatrix}Q_{yz}\\Q_{xz}\end{Bmatrix}=k_s\int_{-h/2}^{h/2}\begin{Bmatrix}\sigma_{yz}\\\sigma_{xz}\end{Bmatrix}dz \qquad (12)$$

$$\begin{Bmatrix}N_{xx}\\N_{yy}\\N_{xy}\\M_{xx}\\M_{yy}\\M_{xy}\end{Bmatrix}=\begin{bmatrix}A_{11}&A_{12}&0&B_{11}&B_{12}&0\\A_{12}&A_{22}&0&B_{12}&B_{22}&0\\0&0&A_{66}&0&0&B_{66}\\B_{11}&B_{12}&0&D_{11}&D_{12}&0\\B_{12}&B_{22}&0&D_{12}&D_{22}&0\\0&0&B_{66}&0&0&D_{66}\end{bmatrix}\begin{Bmatrix}\varepsilon_x^0\\\varepsilon_y^0\\\gamma_{xy}^0\\\kappa_x\\\kappa_y\\\kappa_{xy}\end{Bmatrix};\begin{Bmatrix}Q_{yz}\\Q_{xz}\end{Bmatrix}=k_s\begin{bmatrix}A_{44}&0\\0&A_{55}\end{bmatrix}\begin{Bmatrix}\gamma_{yz}^0\\\gamma_{xz}^0\end{Bmatrix}$$

where

$$\begin{cases}\left(A_{ij},B_{ij},D_{ij}\right)=\int_{-h/2}^{h/2}Q_{ij}\left(1,z,z^2\right)dz; & (ij)=11,\ 12,\ 21,\ 22,\ 66\\ A_{ij}=\int_{-h/2}^{h/2}Q_{ij}dz; & (ij)=44,\ 55\end{cases} \qquad (13)$$

and k_s denotes the transverse shear correction coefficient which is taken to be k_s = 5/6. The temperature is assumed to only vary along the thickness direction of the shell, thus, $\tau_{xy}=0$. The thermoelastic constitutive for the FG shell in the *x, y* directions are expressed as follows:

$$\sigma_{xx}^{(T)}=\sigma_{yy}^{(T)}=-\frac{E(z,T)\alpha(z,T)}{1-\nu}\Delta T \qquad (14)$$

where, $\Delta T=T(z)-T_0$ is the temperature increase from the reference temperature T_0 at which there are no thermal strains.

The equations of motion using the Hamilton's principle can be written as (Wattanasakulpong and Chaikittiratana, 2015):

$$\frac{\partial N_{xx}}{\partial x}+\frac{\partial N_{xy}}{\partial y}+\frac{Q_{xz}}{R_x}=A_{11}^T\frac{\partial^2 u_0}{\partial x^2}+A_{22}^T\frac{\partial^2 u_0}{\partial y^2}+B_{11}^T\frac{\partial^2\phi_x}{\partial x^2}+B_{22}^T\frac{\partial^2\phi_x}{\partial y^2}+I_0\frac{\partial^2 u_0}{\partial t^2}+I_1\frac{\partial^2\phi_x}{\partial t^2}$$

$$\frac{\partial N_{xy}}{\partial x}+\frac{\partial N_{yy}}{\partial y}+\frac{Q_{yz}}{R_y}=A_{11}^T\frac{\partial^2 v_0}{\partial x^2}+A_{22}^T\frac{\partial^2 v_0}{\partial y^2}+B_{11}^T\frac{\partial^2\phi_y}{\partial x^2}+B_{22}^T\frac{\partial^2\phi_y}{\partial y^2}+I_0\frac{\partial^2 v_0}{\partial t^2}+I_1\frac{\partial^2\phi_y}{\partial t^2}$$

$$\frac{\partial Q_{xz}}{\partial x}+\frac{\partial Q_{yz}}{\partial y}-\frac{N_{xx}}{R_x}-\frac{N_{yy}}{R_y}=A_{11}^T\frac{\partial^2 w_0}{\partial x^2}+A_{22}^T\frac{\partial^2 w_0}{\partial y^2}+I_0\frac{\partial^2 w_0}{\partial t^2} \qquad (15)$$

$$\frac{\partial M_{xx}}{\partial x}+\frac{\partial M_{yy}}{\partial y}-Q_{xz}=B_{11}^T\frac{\partial^2 u_0}{\partial x^2}+B_{22}^T\frac{\partial^2 u_0}{\partial y^2}+D_{11}^T\frac{\partial^2\phi_x}{\partial x^2}+D_{22}^T\frac{\partial^2\phi_x}{\partial y^2}+I_1\frac{\partial^2 u_0}{\partial t^2}+I_2\frac{\partial^2\phi_x}{\partial t^2}$$

$$\frac{\partial M_{xy}}{\partial x}+\frac{\partial M_{yy}}{\partial y}-Q_{yz}=B_{11}^T\frac{\partial^2 v_0}{\partial x^2}+B_{22}^T\frac{\partial^2 v_0}{\partial y^2}+D_{11}^T\frac{\partial^2\phi_y}{\partial x^2}+D_{22}^T\frac{\partial^2\phi_y}{\partial y^2}+I_1\frac{\partial^2 v_0}{\partial t^2}+I_2\frac{\partial^2\phi_y}{\partial t^2}$$

where,

$$\begin{cases} (A_{11}^T, B_{11}^T, D_{11}^T) = \int_{-h/2}^{h/2} \sigma_{xx}^{(T)}(1,\ z,\ z^2).dz \\ A_{22}^T = A_{11}^T; B_{22}^T = B_{11}^T; D_{22}^T = D_{11}^T \\ I_i = \int_{-h/2}^{h/2} \rho(z).z^i.dz \quad i=(0,\ 1,\ 2) \end{cases} \quad (16)$$

By substituting the force resultants, total moment resultants, and transverse force resultants in Eq. (15) with those of Eq. (12), the governing equations for the FG doubly curved shell are obtained in terms of the displacement variables of Eqs. (15).

3. ANALYTICAL SOLUTION

Based on Navier's approach, the displacement unknowns satisfying the simply supported boundary conditions for the FG doubly-curved shell panel can be expressed in the following forms:

$$\begin{Bmatrix} u_0(x,y,t) \\ v_0(x,y,t) \\ w_0(x,y,t) \\ \phi_x(x,y,t) \\ \phi_y(x,y,t) \end{Bmatrix} = \sum_{m=1}^{\infty}\sum_{n=1}^{\infty} \begin{Bmatrix} u_{mn}e^{i\omega t}\cos(\alpha x)\sin(\beta y) \\ v_{mn}e^{i\omega t}\sin(\alpha x)\cos(\beta y) \\ w_{mn}e^{i\omega t}\sin(\alpha x)\sin(\beta y) \\ \phi_{xmn}e^{i\omega t}\cos(\alpha x)\sin(\beta y) \\ \phi_{ymn}e^{i\omega t}\sin(\alpha x)\cos(\beta y) \end{Bmatrix} \quad (17)$$

where u_{mn}, v_{mn}, w_{mn}, ϕ_{xmn}, ϕ_{ymn} are the unknown coefficients; i is the imaginary unit ($i^2 = -1$); ω is the natural frequency; $\alpha = m\pi/a; \beta = n\pi/b;$

A simplified form of the equation of motion can be obtained by substituting Eq. (17) into the terms of displacement variables of Eq. (15) to obtain

$$\left([K]_{5\times5} - \omega^2[M]_{5\times5}\right)\{\Delta\}_{5\times1} = \{0\}_{5\times1} \quad (18)$$

where

$$[B_i^m] = \begin{bmatrix} N_{i,x} & 0 & 0 & 0 & 0 \\ 0 & N_{i,y} & 0 & 0 & 0 \\ N_{i,y} & N_{i,x} & 0 & 0 & 0 \end{bmatrix}; \quad [B_i^b] = \begin{bmatrix} 0 & 0 & N_{i,x} & 0 & 0 \\ 0 & 0 & 0 & 0 & N_{i,y} \\ 0 & 0 & 0 & N_{i,y} & N_{i,x} \end{bmatrix};$$

$$[B_i^s] = \begin{bmatrix} 0 & 0 & N_{i,x} & N_i & 0 \\ 0 & 0 & N_{i,y} & 0 & N_i \end{bmatrix} \quad (24)$$

$[K]_{5x5}$ and $[M]_{5x5}$ are the stiffness matrix and the mass matrix, respectively. K_{ij} and M_{ij} are the elements which can be obtained by the Symbolic Toolbox using the Matlab software. $\{\Delta\}_{5x1} = \{u_{mn}\ v_{mn}\ w_{mn}\ \phi_{xmn}\ \phi_{ymn}\}^T$

The natural frequency, ω_{mn}, can be obtained by solving the above eigenvalue type equation (Eq. 18). With each pair of m and n, there is a corresponsive unique mode shape of the natural frequency for the FG doubly-curved shell.

4. FINITE ELEMENT MODEL

When the nine-nodded isoparametric quadratic element is adopted and the interpolation formulated, the spatial coordinates are:

$$x = \sum_{i=1}^{9} N_i x_i \ ; \ y = \sum_{i=1}^{9} N_i y_i \quad (19)$$

where N_i is the quadratic shape function.

The displacement vector $\{u\}$ at any point (x, y, 0) on the mid-plane is defined in terms of nodal variables via the shape function matrix $[N]$ as

$$\{u\} = [N]\{u_i\} \quad (20)$$

where $\{u\} = \begin{bmatrix} u_0 & v_0 & w_0 & \theta_x & \theta_y \end{bmatrix}^T$ (21)

In which $\{u_i\}$ is the nodal displacement vector of element i. From equations (20) and (21) the reduced strain vector $[\tilde{\varepsilon}]$ can be written as

$$\{\tilde{\varepsilon}\} = [B]\{u_i\} \quad (22)$$

where $[B] = \begin{bmatrix} [B_1] & [B_2] & \dots & [B_9] \end{bmatrix}$ (23)

with

In which $N_{i,x}$ and $N_{i,y}$ are the derivatives of the shape functions in the x and y directions, respectively (i = 1, 2, …, 9).

Substituting strains and stresses into Hamilton's variational principle, we get the elementary governing equation of motion as follows:

$$[M_e]\{\ddot{q}_e\} + [K_e]\{q_e\} = \{F_e\} \quad (25)$$

where

$[M_e] = \int_A N^T m N \, dA$ is the consistent mass matrix,

$[K_e] = \int_A [B]^T [D][B] \, dA$ is the element stiffness matrix, and

$\{F_e\} = \int_A N^T p \, dA$ is the nodal load vector.

In which

$$m = \rho t \begin{bmatrix} 1 & 0 & 0 & 0 & 0 \\ 0 & 1 & 0 & 0 & 0 \\ 0 & 0 & 1 & 0 & 0 \\ 0 & 0 & 0 & \frac{t^2}{12} & 0 \\ 0 & 0 & 0 & 0 & \frac{t^2}{12} \end{bmatrix}$$

Transformation into the global coordinate system can be obtained by

$$\left[M_G^e\right] = [T]^T [M_e][T]$$

$$\left[K_G^e\right] = [T]^T [K_e][T]$$

$$\left\{F_G^e\right\} = [T]^T \{F_e\}$$

where $[T]$ is the local-global transformation matrix.

Assembling the elements, we get the final governing equation of motion:

$$[M_G]\{\ddot{q}\} + [K_G]\{q\} = \{F_G\} \quad (26)$$

For free harmonic vibrations and considering the n^{th} mode, Eq. (26) can be written as

$$\left([K_G] - \omega_n^2 [M_G]\right)\{q\} = 0$$

where ω_n is the natural frequency of mode n.

5. NUMERCIAL EXAMPLES AND RESULTS

5.1. Comparison study

In order to verify the accuracy of the present solutions, the non-dimensional frequencies of the FG plate, and the cylindrical, spherical and hyperbolic shell panels were calculated by the analytical (FSDT) and finite element (FEM) models. It should be noted that the doubly-curved shallow shell can be flexibly degenerated into the different structures by setting these quantities.

- $\frac{a}{R_x} = \frac{b}{R_y} = 0$ for the plate structures; $\frac{a}{R_x} = 0$ for the cylindrical panel (CYL);
- $\frac{a}{R_x} = \frac{b}{R_y} \neq 0$ for the spherical panel (SPH); $\frac{b}{R_y} = -\frac{a}{R_x} \neq 0$ for the hyperbolic paraboloidal panel (HYP).

Based on Reddy & Chin (1998), the material properties used in the present study are listed in Table 1.

Example 1:

The non-dimensional frequencies ($\Omega_1 = \omega h \sqrt{\rho_c / E_c}$) of the FG plate and shells under ambient temperatures were calculated as shown in Table 2, and these obtained results were compared with Matsunaga's (2008) using the method of power series expansion of displacement components. The geometrical parameters of the simply supported doubly-curved shell panel were: a/b = 1 and a/h = 10. The FG structures were made from a mixture of ceramic (Al_2O_3) and metal (Al). The temperature independent properties of these materials were as follows

- Ceramic-Al_2O_3: E_c = 380 GPa; ρ_c = 3800 kg/m^3; ν = 0.3

- Metal (Al): E_m = 70 GPa; ρ_m = 2702 kg/m^3; ν = 0.3

Table 1. Temperature-dependent coefficients for ceramic and metal

Material	Properties	P_0	P_{-1}	P_1	P_2	P_3
Si_3N_4	E_c (Pa)	3.4843E+11	0	-3.07E+04	2.16E+07	-8.946E-11
	α_c (1/K)	5.8723E-06	0	9.095E-04	0	0
	K_c (W/m K)	13.723	0	-1.032E-03	5.466E-07	-7.876E-11
	v_c	0.24	0	0	0	0
	ρ_c (kg/m^3)	2370	0	0	0	0
SUS304	E_m (Pa)	2.0104E+11	0	3.079E-04	-6.53E-07	0
	α_m (1/K)	1.233E-05	0	8.086E-04	0	0
	K_m (W/m K)	15.379	0	-1.264E-03	2.09E-06	-7.223E-10
	v_m	0.3262	0	-2.002E-04	3.797E-07	0
	ρ_m (kg/m^3)	8166	0	0	0	0

Table 2. Comparison of non-dimensional frequencies for the FG plates and shells under ambient temperatures

Structure	Source	Volume fraction exponent *p*				
		p = 0	p = 0.5	p = 1	p = 4	p = 10
Plate (a/Rx = b/Ry = 0)	Matsunaga (2008)	0.0577	0.0492	0.0443	0.0381	0.0364
	Present (Analytical)	0.0577	0.0490	0.0442	0.0382	0.0366
	Present (FEM)	0.0576	0.0490	0.0442	0.0382	0.0365
	Difference [a] (%)	*0.17*	*0.41*	*0.23*	*0.26*	*0.27*
Cylindrical shell panel (a/Rx = 0; b/Ry = 0.5)	Matsunaga (2008)	0.0622	0.0535	0.0485	0.0413	0.0390
	Present (Analytical)	0.0617	0.0527	0.0477	0.0407	0.0385
	Present (FEM)	0.0630	0.0539	0.0489	0.0418	0.0395
	Difference [a] (%)	*1.29*	*0.75*	*0.82*	*1.21*	*1.28*
Spherical shell panel (a/Rx = b/Ry = 0.5)	Matsunaga (2008)	0.0751	0.0657	0.0600	0.0503	0.0464
	Present (Analytical)	0.0746	0.0646	0.0588	0.0491	0.0455
	Present (FEM)	0.0761	0.0661	0.0603	0.0507	0.0469
	Difference [a] (%)	*1.33*	*0.61*	*0.50*	*0.80*	*1.08*
Hyperbolic paraboloidal shell panel (a/Rx = 0.5; b/Ry = - a/Rx)	Matsunaga (2008)	0.0563	0.0479	0.0432	0.0372	0.0355
	Present (Analytical)	0.0548	0.0465	0.0420	0.0363	0.0347
	Present (FEM)	0.0581	0.0494	0.0446	0.0385	0.0369
	Difference [a] (%)	*3.16*	*3.05*	*3.34*	*3.61*	*3.91*

Note: * *Difference* [a] $= 100\%\left[\Omega_1(Matsunaga\ (2008))-\Omega_1(Present\ (FEM))\right]$

As shown in Table 2, the present results obtained by the two solutions above agree well with those used in comparison.

Example 2:

The geometrical parameters of the FG plate in the thermal environment were considered: h = 0.025 m; a/b = 1; a = 0.2 m; and Poisson's ratio ν was taken to be a constant 0.28. The

Table 3. Comparison of non-dimensional frequencies Ω_2 for a simply supported Si_3N_4/SUS304 square plate with different values of the volume fraction index in a thermal environment

p	Source	(m, n)		
		(1, 1)	(1, 2)	(2, 2)
0	Shen and Wang (2012)	12.424	29.192	44.245
	Present (FSDT)	12.440	29.096	43.974
	Present (FEM)	12.207	28.560	43.156
	Difference [b] (%)	1.75	2.16	2.46
0.5	Shen and Wang (2012)	8.607	20.214	30.633
	Present (FSDT)	8.576	20.038	30.275
	Present (FEM)	8.417	19.689	29.748
	Difference [b] (%)	2.21	2.60	2.89
1	Shen and Wang (2012)	7.556	17.726	26.842
	Present (FSDT)	7.520	17.567	26.537
	Present (FEM)	7.383	17.270	26.091
	Difference [b] (%)	2.28	2.57	2.80
2	Shen and Wang (2012)	6.785	15.877	23.994
	Present (FSDT)	6.754	15.770	23.811
	Present (FEM)	6.636	15.515	23.429
	Difference [b] (%)	2.19	2.28	2.35
10	Shen and Wang (2012)	5.878	13.708	20.660
	Present (FSDT)	5.846	13.649	20.602
	Present (FEM)	5.761	13.459	20.313
	Difference [b] (%)	1.99	1.81	1.68

*Note: * Difference b* = $100\%\left[\Omega_2(Shen\&Wang\ (2012))\text{-}\Omega_2(Present\ (FEM))\right]$

temperature on the top and bottom surfaces of the plate were assumed to be T_c = 400K and T_m = 300K, respectively.

The effective material properties for the selected FGMs are listed in Table 1. The non-dimensional frequency for a Si_3N_4/SUS304 plate were calculated and compared with those from Shen and Wang's (2012) in Table 3, in which

$$\Omega_2=\omega\left(a^2/h\right)\sqrt{\rho_{0m}\left(1-\nu^2\right)/E_{0m}}$$

and ρ_{0m} and E_{0m} were the reference values of ρ_m and E_m at T_0 = 300K. It can be seen clearly that the differences of the non-dimensional frequencies of the two present solutions (Analytical and FEM) match well with those of Shen and Wang (2012).

Thus, Table 2 and Table 3 show that the numerical results obtained in this paper are highly reliable.

In the next section, the investigations presented used both the analytical and numerical results to analyze some parametric studies on the free vibration of the FG plate and doubly-curved shell panels in a thermal environment. The boundary condition was simple support for all cases. Young's modulus and the thermal expansion coefficient of the materials were assumed to be temperature dependent and listed in Table 1, in which the metal was SUS304 and the ceramic was Si_3N_4. Poisson's ratio ν was taken to be a constant 0.28. The non-dimensional natural frequency used was

$\Omega_3 = 100.\omega.h.\sqrt{\rho_{0c}/E_{0c}}$, and ρ_{0c} and E_{0c} were the reference values of ρ_c and E_c at $T_0 = 300K$.

5.2. Parametric study

5.2.1. Effect of the temperature on the non-dimensional fundamental frequencies

Figure 2 depicts the variability of the non-dimensional fundamental frequencies for the FG

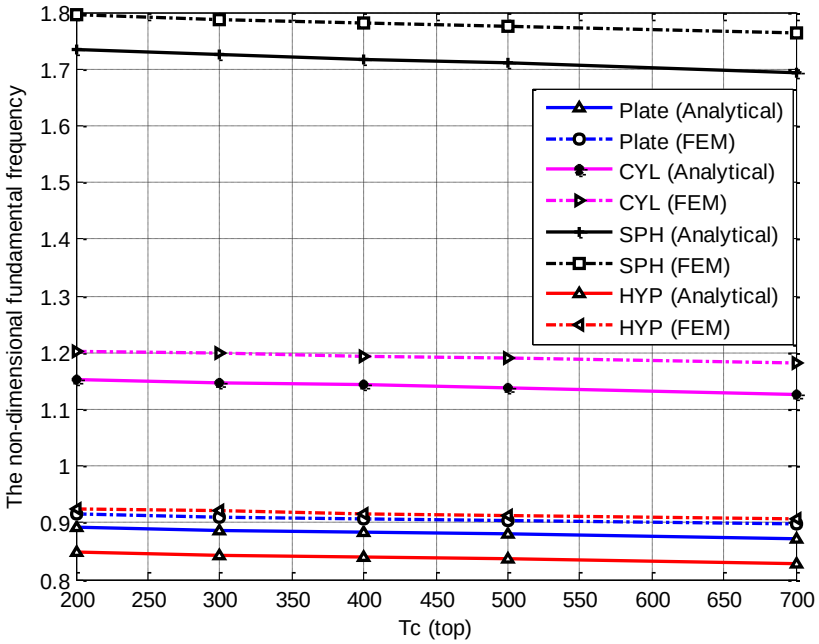

Fig. 2. Effect of the temperature field on the fundamental frequencies of the FG shell panels

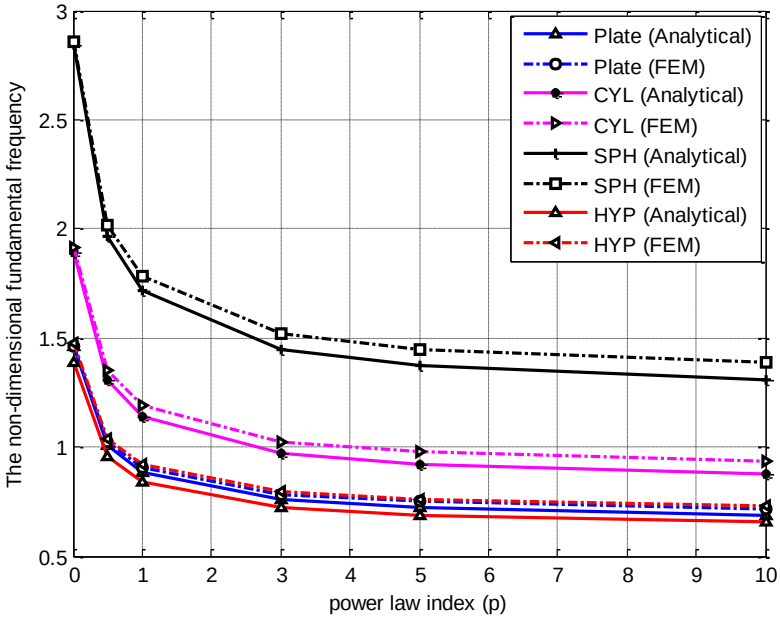

Fig. 3. Effect of the volume fraction index *p* on the fundamental frequencies of the FG shell panels

cylindrical panel and the spherical panel under a thermal environment. The geometric properties were assumed to be a/b = 1; a/h = 20; p = 1; T_m = 300K, and T_c was variable, and with plate ($a/R_x = b/R_y = 0$), cylindrical shell ($a/R_x = 0$; $b/R_y = 0.5$), spherical shell ($a/R_x = b/R_y = 0.5$), and hyperbolic paraboloidal shell ($a/R_x = 0.5$; $b/R_y = - a/R_x$).

According to the Fig. 2, the non-dimensional fundamental frequencies of the plate and panels decreased moderately when the temperature of the ceramic surface (T_c) increased. The reason for the reduction of the non-dimensional fundamental frequencies can be explained by the fact that the stiffness of the shell panel decreased dramatically when the temperature increased.

5.2.2. Effect of the power law index on the natural fundamental frequency

In order to study the effect of the volume fraction index *p* on the non-dimensional fundamental frequency of the FG plate and shell panels, for an example, the geometric properties of the shell panels and the temperature were denoted as a/b = 1, a/h = 20, T_m = 300K, and T_c = 400K. The side to radius ratio was set as follows: for the plate: $a/R_x = b/R_y = 0$, for the cylindrical panel (CYL): $a/R_x = 0$; $b/R_y = 0.5$, for thespherical panel: (SPH): $a/R_x = b/R_y = 0.5$, and for the hyperbolic paraboloidal panel (HYP): $a/R_x = 0.5$; $b/R_y = - a/R_x$.

Fig. 3 shows the results that as the volume fraction index (p) incrementally increased, the non-dimensional fundamental frequency reduced dramatically for all structures of the plate and shell panels. The reason for this can be explained in that when the volume fraction index (p) increased, the ceramic constituent of the material reduced, therefore, the stiffness of the shell panels decreased. As a consequence, the non-dimensional fundamental frequency also decreased. Moreover, the results depicted in Fig. 3 imply an important aspect for FGMs having their properties inbetween the two extreme limits of metal and ceramic.

5.2.3. Effect of thickness on the natural fundamental frequencies

In this section, FG shell panels with a/b = 1 and p = 1 were considered to study the effect of the side-to-thickness ratio (varying a/h from 20 to 200) on the non-dimensional fundamental frequencies under the influence of a temperature field of T_m = 300 K and T_c = 400 K. The geometrical parameters of the shell panels were: with the cylindrical panel (CYL) $a/R_x = 0$, $b/R_y = 0.5$; the spherical panel (SPH) $a/R_x = b/R_y = 0.5$, and the hyperbolic paraboloidal panel (HYP) ($a/R_x = 0.5$; $b/R_y = - a/R_x$). The results are shown in the Fig. 4.

It can be observed from Fig. 4 that when the side-to-thickness ratio (a/h) increased, the non-dimensional fundamental frequency of the present structures decreased. The explanation for this is that when the ratio a/h increased, the shell panel became thinner, thus, the stiffness of the shell decreased. This means that the non-dimensional fundamental frequency of the shell panel also decreased.

From Figs. 2-4, it can be seen that the non-dimensional fundamental frequencies of the spherical panels were always higher than those of the cylindrical panels and hyperbolic paraboloidal panels. This leads one to believe that the stiffness of the spherical panel was the highest of the all considered structures.

6. CONCLUSION

Based on the first-order shear deformation theory, an analytical solution and finite element models using a nine-noded isoparametric quadratic element were performed for the free vibration analysis of simply supported functionally graded plate and shell panels, namely, cylindrical, spherical and hyperbolic paraboloid. It is obvious that the results obtained are in good agreement with those of previously described methods and solutions. According to this investigation, the results presented in the figures reveal the following:

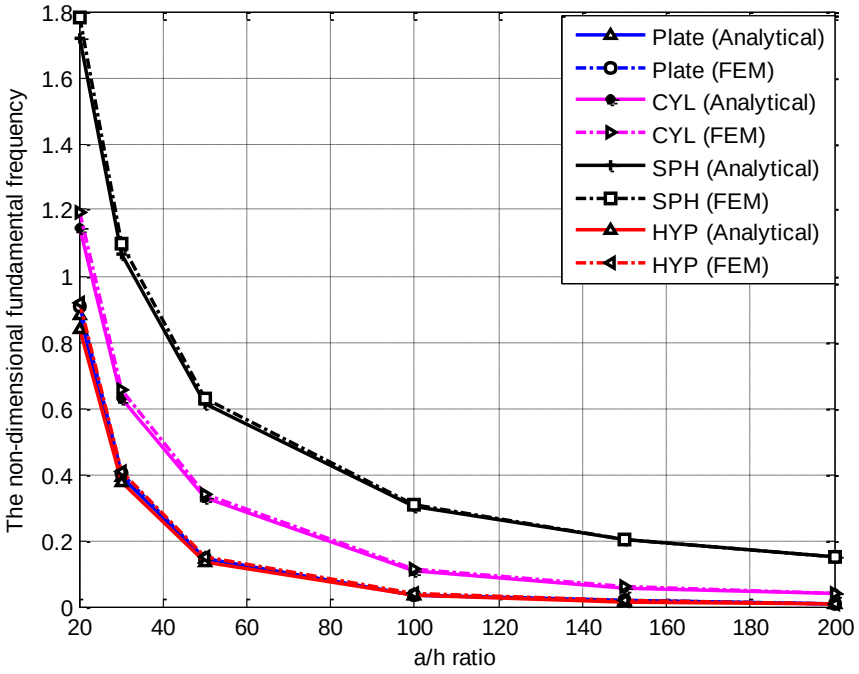

Fig. 4. Effect of a/h ratio on the fundamental frequencies of the FG shell panels

- The non-dimensional fundamental frequencies of the plate and shell panels decreased with increases of the temperature field (T_c), volume fraction index (p) and side-to-thickness ratio (a/h);

- The non-dimensional fundamental frequencies of the spherical panel were the highest of all considered structures.

REFERENCES

Alijani, F., M. Amabili, and F. Bakhtiari-Nejad (2011). Thermal effects on nonlinear vibrations of functionally graded doubly curved shells using higher order shear deformation theory. Composite Structures, 93(10): 2541-2553.

Bhangale, R.K., N. Ganesan, and C. Padmanabhan (2006). Linear thermoelastic buckling and free vibration behavior of functionally graded truncated conical shells. Journal of Sound and Vibration, 292(1): 341-371.

Dong, D. T., & Van Dung, D. (2017). A third-order shear deformation theory for nonlinear vibration analysis of stiffened functionally graded material sandwich doubly curved shallow shells with four material models. Journal of Sandwich Structures & Materials, 1099636217715609.

Duc, N. D., Quang, V. D., & Anh, V. T. T. (2017). The nonlinear dynamic and vibration of the S-FGM shallow spherical shells resting on an elastic foundations including temperature effects. International Journal of Mechanical Sciences, 123: 54-63.

Haddadpour, H., S. Mahmoudkhani, and H. Navazi (2007). Free vibration analysis of functionally graded cylindrical shells including thermal effects. Thin-walled Structures, 45(6): 591-599.

Huang, X.-L. and H.-S. Shen (2004). Nonlinear vibration and dynamic response of functionally graded plates in thermal environments. International Journal of Solids and Structures, 41(9): p. 2403-2427.

Javaheri, R. and M. Eslami (2002). Thermal buckling of functionally graded plates. AIAA Journal, 40(1): 162-169.

Kadoli, R. and N. Ganesan (2006). Buckling and free vibration analysis of functionally graded cylindrical shells subjected to a temperature-specified boundary condition. Journal of Sound and Vibration, 289(3): 450-480.

Malekzadeh, P. and Y. Heydarpour (2012). Free vibration analysis of rotating functionally graded cylindrical shells in thermal environment. Composite Structures, 94(9): 2971-2981.

Matsunaga, H. (2008). Free vibration and stability of functionally graded shallow shells according to a 2D higher-order deformation theory. Composite Structures, 84(2): 132-146.

Pradyumna, S. and J. Bandyopadhyay (2010). Free vibration and buckling of functionally graded shell panels in thermal environments. International Journal of Structural Stability and Dynamics, 10(05): 1031-1053.

Quan, T. Q., & Dinh Duc, N. (2016). Nonlinear vibration and dynamic response of shear deformable imperfect functionally graded double-curved shallow shells resting on elastic foundations in thermal environments. Journal of Thermal Stresses, 39(4): 437-459.

Shen, H.-S. and Z.-X. Wang (2012). Assessment of Voigt and Mori-Tanaka models for vibration analysis of functionally graded plates. Composite Structures, 94(7): 2197-2208.

Sheng, G. and X. Wang (2010). Thermoelastic vibration and buckling analysis of functionally graded piezoelectric cylindrical shells. Applied Mathematical Modelling, 34(9): 2630-2643.

Wattanasakulpong, N. and A. Chaikittiratana (2015). An analytical investigation on free vibration of FGM doubly curved shallow shells with stiffeners under thermal environment. Aerospace Science and Technology, 40: 181-190.

Yang, J. and H. S. Shen (2001). Dynamic response of initially stressed functionally graded rectangular thin plates. Composite Structures, 54: 457-508.

Zhao, X., Y. Lee, and K.M. Liew (2009). Thermoelastic and vibration analysis of functionally graded cylindrical shells. International Journal of Mechanical Sciences, 51(9): 694-707.